Empirical models for predicting water and heat flow properties of permafrost soils

Michael T. O'Connor[1*], M. Bayani Cardenas[1*], Stephen B. Ferencz[1],
Yue Wu[2], Bethany T. Neilson[3], Jingyi Chen[2], and George W. Kling[4]

[1] Dept. of Geological Sciences, The University of Texas at Austin, Austin, TX

[2] Dept. of Aerospace Engineering and Engineering Mechanics, The University of Texas at Austin, Austin, TX

[3] Dept. of Civil Engineering, Utah State University, Logan, UT

[4] Dept. of Ecology and Evolutionary Biology, University of Michigan, Ann Arbor, MI

* Joint corresponding authors: Michael O'Connor, mtoconnor12@gmail.com ; M. Bayani Cardenas, cardenas@jsg.utexas.edu

Key Points

(1) Thermal and hydraulic properties of 265 permafrost soil samples from across the Arctic Foothills of Alaska were measured.

(2) Different soil strata (acrotelm, catotelm, and mineral soil) have consistent properties and thickness over hundreds of kilometers.

(3) The soil properties are strongly related to vegetation and surface slope, and can be independently predicted from soil bulk density.

Abstract

Warming and thawing in the Arctic are promoting biogeochemical processing and hydrologic transport in carbon-rich permafrost and soils that transfer carbon to surface waters or the atmosphere. Hydrologic and biogeochemical impacts of thawing are challenging to predict with sparse information on arctic soil hydraulic and thermal properties. We developed empirical and statistical models of soil properties for three main strata in the shallow, seasonally-thawed soils above permafrost in a study area of ~7,500 km^2 in Alaska. The models show that soil vertical stratification and hydraulic properties are predictable based on vegetation cover and slope. We also show that the distinct hydraulic and thermal properties of each soil stratum can be predicted solely from bulk density. These findings fill the gap for a sparsely mapped region of the Arctic and enable regional interpolation of soil properties critical for determining future hydrologic responses and the fate of carbon in thawing permafrost.

Plain Language Summary

Arctic permafrost holds about as much carbon as currently present in the atmosphere. Rapid warming in the Arctic has raised concerns that this stored carbon could thaw, and get released into the atmosphere, which would substantially amplify global warming. The rate of this carbon release to the atmosphere depends on the rate of environmental processes such as microbial respiration and heat and groundwater flow. The soil properties controlling these processes are currently unknown across most of the Arctic, making predictions of the processes highly uncertain at larger scales. This study uses hundreds of measurements of soil properties across an area of land larger than Delaware to show that soil properties in the foothills of the Brooks Range in northern Alaska are predictable if the landscape slope, dominant vegetation type, and local topography are known. This study provides a base for calculating transport processes related to soil carbon in the Arctic.

1. Introduction

More than half of Earth's soil carbon (C) is held in arctic permafrost landscapes [*Hugelius et al.*, 2014; *Ping et al.*, 2008]. As the Arctic warms, substantial amounts of this C could be released as greenhouse gases, creating a positive feedback for global climate warming [*Schaefer et al.*, 2014; *Schuur et al.*, 2015; *Serreze and Barry*, 2011]. However, there is large uncertainty in the amount and timing of permafrost soil C release, with models predicting that the Arctic could be a small net sink or a large net source of C to the atmosphere in the future [*McGuire et al.*, 2018; *Schuur et al.*, 2015].

The prediction uncertainties are related to soil characteristics and hydrological processes that are poorly represented or missing entirely from the models. A survey of uncertainties and data needs of ecosystem models used to predict permafrost or C dynamics indicated large gaps in several soil characteristics related to hydrology; the gaps are related primarily to soil moisture and secondarily to water table depth, evapotranspiration, freeze-thaw dynamics, soil temperature, and soil vertical structure [*Fisher et al.*, 2018]. Another gap concerns below-ground transport of dissolved C from land to surface waters. More than half of permafrost soil C loss over time can be due to lateral soil water flow [*Plaza et al.*, 2019]. This transport of C from land to surface waters and subsequent release as gases to the atmosphere can be equivalent to ~20% of the net, terrestrial C sink in the Arctic [*Kling et al.*, 1991]. A better understanding of soil characteristics related to water and heat flow is necessary to reduce the uncertainties in predicting C losses from thawing permafrost soils [*McGuire et al.*, 2016].

The transport of C and heat in soils is strongly controlled by hydrology. For example, soil permeability in permafrost settings controls groundwater flow rates [*O'Connor et al.,* 2019] and the transport of leached C [*Neilson et al.*, 2018]. Permeability also affects soil moisture, and the production of CH_4 is higher in damp or inundated soils while CO_2 production dominates in drier, better drained soils [*Lawrence et al.*, 2015]. Heat transport through soils is related to soil hydraulic properties [*Sjöberg et al.,* 2016], and it is critical for freeze-thaw dynamics [*Painter et al.,* 2016]. Wet and porous soils effectively transmit and store heat, and will warm more from above and thaw deeper than will dry soils [*Shiklomanov et al.*, 2010; *Harp et al.,* 2016]. Any warm water flowing easily through soils also delivers heat deeper and to downslope areas. In contrast, drier soils have lower thermal conduction because there is less water present that can efficiently transfer heat, and these soils instead provide insulation from surface warming. Finally, the warmer soils will be more biologically and chemically reactive because reaction rates inherently increase with temperature. Thus, the effect of thawing on permafrost soil dynamics and function is determined by connections and feedbacks among water flow, heat flow, and the rates of soil biogeochemical reactions.

Few studies have extensively measured the properties necessary to broadly understand or predict water and heat flow in arctic soils and to meaningfully represent the function of these soils in models [*Hinzman et al.*, 1991; *Quinton et al.*, 2008]. Basic soil properties such as hydraulic conductivity K_H [$L\ T^{-1}$], thermal conductivity K_T [$W\ m^{-1}\ K^{-1}$], porosity ϕ [-], dry bulk density ρ_b, [$M\ L^{-3}$], and the water retention and transmission capacity of variably saturated soils represented by the van Genuchten α [L^{-1}] and n [-] parameters [*van Genuchten*, 1980], are very rarely simultaneously measured, especially systematically across a region. Mechanistic modeling studies of areas spanning local to regional coverage have shown that these soil properties are the most important parameters to know in order to predict long-term thawing [*Harp et al.*, 2016; *Jafarov and Schaefer*, 2016]; however, such modeling-based sensitivity analyses are constrained by too little or no data on the aforementioned properties. Because the most important parameters are not known, they are just used as a fitting parameter in models of heat and water flow. Soil properties are typically used as calibration parameters in models in order to match temperature observations [*Nicolsky et al.*, 2009]. In addition to the need for accurate and meaningful models of heat and water flow, biogeochemical processes modeling is also critical. Observational studies of hydrology-dependent biogeochemical processes in the Arctic have mostly been small-scale [*Kling et al.*, 2014]. Transferring findings from both theoretical and empirical local studies to regional and global scales continues to be a challenge because of the knowledge gaps above. The gaps in data and approaches to scaling up create large uncertainties. Because economic damages from thawing permafrost are estimated in the tens of trillions of dollars [*Hope and Schaefer*, 2016; *Yumashev et al.*, 2019], reducing this uncertainty by filling the gaps is paramount.

2. Methods

The goal of this study is to develop observation-based models for predicting soil water and heat flow properties that are broadly applicable across large parts of the Arctic. This is achieved by terrain analysis and field and lab soil measurements collected from 265 sites distributed across ~7,500 km^2 of the North Slope region of arctic Alaska (Fig. 1). We analyzed how soil thermal and hydraulic properties vary within each of three main soil strata (see Fig. 1c) which are: acrotelm (living portion of the peat or organic layer), catotelm (dead or ancient peat), and mineral soil. In turn, these soil properties and strata were related with more accessible or more easily-measured variations in land surface characteristics such as vegetation, slope, and microtopographic position. These land surface traits were integrated into a hierarchical and categorical landscape classification scheme. Parsimonious statistical models were used to relate the thermal and hydraulic properties with soil stratification, landscape categories, and easier-to-measure soil bulk density.

2.1. The study area

We conducted studies in the Colville River, Kuparuk River, and Sagavanirktok River watersheds (Fig. 1) during summers from 2017 to 2019. The three study watersheds drain ~60% of the Arctic Foothills of Alaska. The Arctic Foothills ecoregion, which covers a large area (~125,000 km^2) and is defined largely by topography, contains moderate to steep rolling hills carved by several distinct glaciations in the Pleistocene [*Hamilton*, 1982]. It is bounded to the south by the Brooks Range and to the north by the much flatter Arctic Coastal Plain leading to the Arctic Ocean (Fig. 1).

2.2. Mapping and differentiating soil stratification

Soil stratification was determined at 265 locations (Fig. 1, Table S1) by measuring the vertical thickness of three main strata (acrotelm, catotelm, and mineral soil) found in organic-rich or peat soils, typical of those in the region. At each site, an approximately 30×30 cm square section of soil was extracted using a serrated knife and then returned after description and subsampling by coring (Fig. 1c). The boundaries between acrotelm, catotelm, and mineral soil layers were determined using multiple field criteria that are described further in the supplementary text S1.1. Statistical tests were used to determine differences in soil stratification among the three soil strata. Differences were considered 'significant' when the p-value was less than 0.05 and 'substantial' when the differences are obvious qualitatively, but were not statistically significant.

2.3. Classification of sample sites based on landscape traits

A hierarchical classification scheme that combined three easily-identified land surface properties - slope, dominant vegetation type, and microtopographic position (whether the site is at a local high or low point over decimeter scales) - was implemented. Based on the classification used by *Walker and Walker* [1996], the surface slope was used to identify a landscape zone as either 'Hillslope' (steep) or 'Riparian' (relatively flat river valleys). Riparian zones are flatter areas (<10% slope) that border surface streams, while Hillslope zones are steeper areas (>10% slope) which are typically upslope of Riparian zones, when the latter is present. These two zones comprise ~ 90% of the study site used by *Walker and Walker* [1996] as representative of the Arctic Foothills.

The dominant vegetation type was identified within each landscape zone. Substantial work has identified and classified vegetation types within the Toolik Lake Region [*Walker and Walker*, 1996; *Walker et al.*, 2018], the North Slope [*Payne*, 2013], and in arctic continuous permafrost terrain in general [*Stow et al.*, 2004]. Different vocabulary has been used across disciplines to describe different classifications and sub-classifications of this landscape. Here we used four umbrella vegetation types based on common, straightforward criteria to simplify the various sub-classifications. We used 'Sedge' to describe any wet to saturated, graminoid-dominated site; 'Shrub' to describe any site dominated by plants with woody stems (i.e., birch, willow, and alder); 'Tussock' to describe any site dominated by tussock forming sedges (e.g., "cottongrass", genus *Eriophorum*), and 'Sparse Vegetation' to describe any plot with matted lichen vegetation or bare ground. These four types include all the dominant land cover types in the Arctic Foothills (see supplementary text S1.2 for further details).

Next, the landscape zones and vegetation types were combined to produce five categories at the finest-scale classification: (1) hillslope shrub, (2) hillslope tussock, (3) hillslope sedge, and (4) riparian shrub and (5) riparian sedge (Fig. 2). Hillslope sedge corresponds to so-called water tracks, which are zero-order linear drainage features that funnel substantial water flows from hillslopes, are spaced somewhat regularly in intervals of tens of meters, have narrow widths (1 to 3 m), and occur in subtle topographic lows within the landscape [*McNamara et al.*, 1997].

Finally, microtopographic position, whether it was high or low, was established visually by comparing the local elevation of the sample site to the surrounding elevation points. However, microtopography was not discernible in all landscape zones and vegetation types; hence its addition as a criterion was not uniformly applied (see supplementary text S1.3 for further details). Overall, the hierarchical classification resulted in two landscape zones, four vegetation types, five categories that combine landscape zones and vegetation types, and two microtopographic groups.

2.4. Laboratory measurements of soil hydraulic and thermal properties

Soil cores of 5 cm diameter were taken from a subset of sample sites for laboratory analysis. Tests for hydraulic conductivity K_H, thermal conductivity K_T, porosity ϕ, and bulk density (ρ_b) were conducted on each core. For a further subset of sites, we measured moisture-dependent K_T, K_H and soil water tension, i.e., we developed soil moisture retention curves. Using these observations, we analyzed for the parameters α, n, residual water content θ_r, and saturated water content θ_s (which equals ϕ) of the van Genuchten model [*van Genuchten*, 1980]. The van Genuchten model describes how K_H and soil tension are non-linearly related with soil volumetric water content θ. The measurement procedures are described further in supplementary text S1.4.

2.5. Testing differences in soil stratification and properties across landscape classification criteria

The observations were grouped into populations based on the landscape-defined criteria of landscape zones, vegetation types, and combined landscape-vegetation categories (Fig. 2). A one-sample Kolmogorov-Smirnov test was implemented on each dataset to confirm normal distribution of the data. A series of one-way ANOVA and t-tests were then performed to determine if the variability in acrotelm thickness, catotelm thickness, K_H, K_T, ϕ, α, and n was larger between categories than within categories. The categories tested were: landscape zone (Hillslope vs. Riparian), vegetation category (Sedge vs. Tussock vs. Shrub vs. Sparse Vegetation), microtopography (local high vs. local low), and all classifications together (Tables S3 and S4). These tests allowed us to determine which level in the hierarchical classification exerted the most substantial control on soil properties. No comparisons were done in instances where populations had fewer than five samples. For all analyses, a p-value less than 0.05 denoted statistical significance.

3. Results

Measurements of soil stratification and properties throughout the study area (Figs. 1 and 2, and Tables S1 and S2) indicated two major soil layers, each with two sub-layers, for a total of four distinct strata: organic soils, which are further divided into the upper acrotelm peat and the lower catotelm peat; and mineral soils, divided into an upper mixed organic-mineral loess (organic-rich) and a lower homogeneous loess layer (organic-poor). The terms acrotelm, catotelm, and mineral soil for soil strata, as well as variants of them, have been used to describe peat soils present within arctic permafrost environments [*Hinzman et al.*, 1991; *Neilson et al.*, 2018; *Quinton et al.*, 2008]; soil science investigations have further classified these broad soil types with substantially greater detail (e.g., *Holden and Burt* [2003]). We found remarkable consistency in both the thicknesses of these strata and the thermal and hydraulic properties of the soils that comprise the strata across hundreds of square kilometers of the Arctic Foothills (Fig. 2, Tables S3 and S4).

3.1. Stratum thickness varies based on landscape classification

Landscape zone was significantly related to catotelm thickness, but was unrelated to acrotelm thickness (Fig. 2, Table S3). Vegetation type was related to the different thicknesses characteristic of acrotelm versus catotelm. For example, sites dominated by sedge have significantly thinner acrotelm and significantly thicker catotelm than sites dominated by shrub or tussock. Similarly, while the mean acrotelm thickness of shrub-dominated landscapes is no different from the mean thicknesses of other landscapes, the range of acrotelm thicknesses is substantially larger.

Combining the landscape zone and vegetation type yielded normally-distributed datasets that described the overall stratigraphy of each category (Fig. 2). Hillslope Sedge, which corresponds to sedge-dominated water tracks occurring only in the hillslope zone (e.g., *McNamara et al.* [1997]), has both the thinnest acrotelm (9 cm; see Table S3) and thickest catotelm (19 cm) observed in the hillslope (Fig. 2). Hillslope Shrub sites conversely have the thickest acrotelm and thinnest catotelm, and Hillslope Tussock sites have intermediate acrotelm and catotelm thicknesses overall. However, because tussock sites exhibit substantial microtopography on the order of tens of cm, we measured significant differences in acrotelm thickness between local highs and local lows (Fig. 2). Local highs, which are commonly dry and contain small woody shrubs, have thick acrotelm similar to the Shrub sites, while local lows, which are commonly flooded and populated with sedges and mosses, have relatively thinner acrotelm – this is similar to the pattern observed in the perennially-wet and sedge-dominated water track sites.

The total organic layer thickness across Riparian Zone sites varied substantially based primarily on vegetation type. Tussock vegetation is uncommon in the riparian zone and thus we have no sites in that category. However, we observed substantial differences between the soil stratigraphy underlying sedge and shrub sites in the riparian areas. This difference was largely due to anomalously thick catotelm under sedge vegetation; catotelm layers in riparian sedges are much thicker than the rest of the catotelm strata observed under other vegetation types (Fig. 2, Table S3).

3.2. Soil strata have different and predictable properties

Acrotelm and catotelm soils had well-constrained and normally-distributed physical properties (Fig. 3). While the thermal properties of these two soil types were indistinguishable, their hydraulic properties were distinct. The saturated thermal conductivity (K_T) of both soil types of approximately 0.5-0.6 W m^{-1} K^{-1} is similar to water. This is because both acrotelm and catotelm soils are very porous, with ϕ ranging between 75 and 95% (Figs. 3 and 4), and thus a saturated sample is mostly water. Similarly, the dry K_T of both acrotelm and catotelm soil is quite low (0.07-0.09 W m^{-1} K^{-1}), approaching the thermal conductivity of air.

The high porosities (ϕ) of both acrotelm and catotelm soils, with acrotelm ϕ approaching the highest values observed in nature (Fig. 3 and Table S4), are consistent with values measured in other peat studies [*Beckwith et al.*, 2003]. Although catotelm soils have only slightly lower ϕ, they have significantly lower hydraulic conductivity (K_H) and α. Acrotelm K_H was measured at 0.0013 ± 0.0012 m s^{-1} (std. dev), whereas catotelm K_H is almost 30 times lower (Table S4). Catotelm K_H has a relatively broader range than acrotelm K_H.

Acrotelm soils drain rapidly and retain very little porewater, indicated by larger van Genuchten α values, in comparison to catotelm soils (Fig. 3 and Figs. S1 and S2). While the van Genuchten *n* shape parameter does not vary significantly between soil types (Table S2), α varies over multiple orders of magnitude. Acrotelm α is very high (Fig. 3) in comparison to other soils in the study region and in general (e.g., values reported in *van Genuchten* [1980]).

Overall, mineral soils are more thermally conductive (higher K_T), less porous (lower ϕ), less permeable (lower K_H), and retain more porewater (lower α) than any of the acrotelm or catotelm soils we tested. However, unlike the organic soils, which consistently contained two compositionally and structurally homogeneous layers, the composition and structure of the mineral soils we observed varied substantially (Fig. 3). While many of the mineral soils we sampled were strongly mineral-dominated with less than 5% organic matter (OM) by weight (determined through loss-on-ignition), others contained a substantial amount of organic material (ranging from 10-70%) [*O'Connor*, 2019]. The organic-poor mineral soils (<5% OM) exhibited more constrained and normally-distributed thermal and hydraulic properties, whereas the hydraulic and thermal properties of the transitional, organic-rich, mineral soils (10-70% OM) varied much more.

3.3. Soil bulk density is a universal predictor of soil properties

Soil dry bulk density (ρ_b) correlates well with the other soil properties, regardless of soil layer (Fig. 4). ρ_b can be used to estimate both ϕ and K_T using a linear equation. Bulk density can also be used to estimate hydraulic conductivity K_H and van Genuchten α using power functions. The regression equations using ρ_b as a predictor all explain at least 74% (for α) and up to 90% (for ϕ) of the variance in the soil properties ϕ, K_T, K_H, and α (Fig. 4).

4. Discussion and Concluding Remarks

This study developed landscape-based soil stratigraphy patterns and thermal and hydraulic properties for the foothills of the North Slope of Alaska. Previous studies have used similar landscape-driven approaches to identify patterns in select subsurface properties such as soil texture [*Walker and Everett*, 1991], soil organic thickness [*Bockheim*, 1998], and active layer thickness [*Walker et al.*, 2003]. Here, we developed statistical models of soil thermal and hydraulic soil properties (mean and standard deviation) for soils with different landscape properties such as slope and vegetation type. These models potentially connect remote-sensing products such as the North Slope Science Initiative Land Cover Map [*Payne*, 2013] with soil properties, enabling expansion of predictions to larger regions in the Arctic.

The most general pattern of soil stratification, specifically the occurrence of three main strata (acrotelm, catotelm, and mineral soil) was very consistent across the study area. In addition, the soil thickness of each stratum was strongly related to the landscape properties of slope, vegetation, and in limited cases, microtopographic position (Fig. 2, Table S4). For example, hillslope soils have thinner total organic layers (acrotelm plus catotelm) than riparian soils, because they have on average a thinner catotelm and comparable acrotelm thickness. Microtopographic highs have relatively thicker acrotelm and thinner catotelm than microtopographic lows. Soils under shrub vegetation tend to have thick acrotelm with thin catotelm, and soils under sedges show the opposite tendency (Fig. 2). The strong relationship of stratum thickness to landscape properties was present despite major variations in the glacial age and history of the land surface. The sample sites spanned the surfaces of the younger Itkillik I (~60,000 year BP) and Itkillik II (~12,000 year BP) glaciations, as well as the older Sagavanirktok glaciation (~250,000 year BP) [*Hamilton*, 1982]. However, all tests comparing differences between soil stratification, strata thickness, or soil properties across these different-aged glacial surfaces failed to show significant differences. Glacial age is unimportant for developing classifications of soil properties within the study area.

The flow of heat, water, and dissolved materials in soils is governed by the thickness of strata and their inherent properties such as porosity and conductivity. Within each stratum described above, the measured soil properties were consistent and relatively well-constrained within any landscape category (Fig. 3). Although the distributions of properties among categories have some overlap, the data show that acrotelm soils are substantially more porous and permeable, less dense and thermally conductive, and retain less porewater than do catotelm and especially than mineral soils (Fig. 3). Using a subset of our data, studies predicted that as permafrost thaws the water table depth will exert greater control on fluid flux than will thaw depth [*O'Connor et al.*, 2019], and that the main sources of water and dissolved carbon will be in riparian areas with thick organic layers [*Neilson et al.*, 2018; *O'Connor et al.*, 2019]. Our findings suggest that such local predictions apply to much larger spatial areas of the Alaskan tundra.

The idea that bulk density is a predictor of thermal and hydraulic soil properties (Fig. 4) is a concept has also been observed and proposed by others that studied different areas and types of soils [*Liu and Lennartz*, 2019; *Morris et al.*, 2019; *Tian et al.*, 2019; *Xie et al.*, 2018]. Unlike previous studies, the relationships with bulk density developed here used scores of samples from different strata from locations within a large, contiguous area with heterogeneous land cover.

We conclude that permafrost soil thermal and hydraulic properties can be predicted from vegetation maps and digital elevation models using our landscape classification (Figs. 1, 2) and statistical distributions (Fig. 3). Others have used similar approaches of parameterization of soil properties based on ecotypes in the North Slope region [*Nicolsky et al.*, 2017]. Because the North Slope of Alaska has topography and vegetation common across the Arctic [*Nicolsky et al.*, 2017; *Walker et al.*, 2018], our landscape classification of soil properties may be more circumpolar in application.

Acknowledgments

The authors thank Matthew Kaufman, Eric Guiltinan, Tyler King, and Jason Dobkowski for their help in the field, and the entire Toolik Field Station Support Staff for their help at the research station. Kindra Nicholaides and Zachary Mungia are thanked for their assistance in the lab. We thank Bryan Travis and an anonymous reviewer for their encouraging and constructive comments. This work was funded by the National Science Foundation grants NSF ARC 1204220, DEB 1026843 and 0639805, PLR 1504006, and OPP 1107593, as well as with generous support from The University of Texas at Austin Geology Foundation, the Geological Society of America Student Research Grant program, and the American Geophysical Union Horton Research Grant. Field work in 2018 and 2019 was supported in part by a grant from the NASA Terrestrial Hydrology Program (grant 80NSSC18K0983) to JC, MBC, and GWK. MTO and MBC designed the study with contributions from BTN and GWK. MTO, SBF, MBC, YW, and JC conducted fieldwork. MTO, SBF, YW, JC, KDN, and ZJM analyzed samples in the laboratory. MTO post-processed all the results including the statistical analysis. MTO, MBC, GWK, and BTN wrote the manuscript and MTO and MBC created the figures. All the data used in this manuscript are included as supplements and are publicly available from the Arctic

LTER Data Repository and the NSF-supported Hydroshare Data Repository (https://www.hydroshare.org/resource/57fb518013474806aa4bc18271b07a32/).

References

Beckwith, C. W., A. J. Baird, and A. L. Heathwaite (2003), Anisotropy and depth-related heterogeneity of hydraulic conductivity in a bog peat. I: laboratory measurements, Hydrological Processes, 17(1), 89-101.

Bockheim, J. G., Walker, D. A., Everett, L. R., Nelson, F. E., Shiklomanov, N. I. (1998), Soils and cryoturbation in moist nonacidic and acidic tundra in the Kuparuk River Basin, Arctic Alaska, Arctic and Alpine Research, 30(2), 166-174, doi: 10.1080/00040851.1998.12002888.

Fisher, J. B., et al. (2018), Missing pieces to modeling the Arctic-Boreal puzzle, Environmental Research Letters, 13(2), doi: 10.1088/1748-9326/aa9d9a.

Hamilton, T. D. (1982), A Late Pleistocene Glacial Chronology for the Southern Brooks Range - Stratigraphic Record and Regional Significance, Geological Society of America Bulletin, 93(8), 700-716.

Harp, D. R., A. L. Atchley, S. L. Painter, E. T. Coon, C. J. Wilson, V. E. Romanovsky, and J. C. Rowland (2016), Effect of soil property uncertainties on permafrost thaw projections: a calibration-constrained analysis, Cryosphere, 10(1), 341-358.

Hinzman, L. D., D. L. Kane, R. E. Gieck, and K. R. Everett (1991), Hydrologic and thermal properties of the active layer in the Alaskan Arctic, in Cold Regions Science and Technology, edited, pp. 95-110.

Holden, J., and T. P. Burt (2003), Hydrological studies on blanket peat: the significance of the acrotelm-catotelm model, Journal of Ecology, 91(1), 86-102, doi: 10.1046/j.1365-2745.2003.00748.x.

Hope, C., and K. Schaefer (2016), Economic impacts of carbon dioxide and methane released from thawing permafrost, Nature Climate Change, 6(1), 56-59.

Hugelius, G., J. Strauss, S. Zubrzycki, J. W. Harden, E. A. G. Schuur, C.-L. Ping, L. Schirrmeister, G. Grosse, G. J. Michaelson, C. D. Koven, J. A. O'Donnell, B. Elberling, U. Mishra, P. Camill, Z. Yu, J. Palmtag, and P. Kuhry (2014), Estimated stocks of circumpolar permafrost carbon with quantified uncertainty ranges and identified data gaps, Biogeosciences, 11, 6573-6593, doi:10.5194/bg-11-6573-2014.

Jafarov, E., and K. Schaefer (2016), The importance of a surface organic layer in simulating permafrost thermal and carbon dynamics, Cryosphere, 10(1), 465-475.

Kling, G. W., G. W. Kipphut, and M. C. Miller (1991), Arctic lakes and streams as gas conduits to the atmosphere - implications for tundra carbon budgets, Science, 251(4991), 298-301.

Kling, G. W., et al. (2014), Land-Water Interactions, in, A Changing Arctic: Ecological Consequences for Tundra, Streams, and Lakes, edited by J. E. Hobbie and G. W. Kling, pp. 143-172, Oxford University Press.

Lawrence, D. M., C. D. Koven, S. C. Swenson, W. J. Riley, and A. G. Slater (2015), Permafrost thaw and resulting soil moisture changes regulate projected high-latitude CO_2 and CH_4 emissions, Environmental Research Letters, 10(9).

Leong, E. C., S. Tripathy, and H. Rahardjo (2003), Total suction measurement of unsaturated soils with a device using the chilled-mirror dew-point technique, Geotechnique, 53(2), 173-182.

Liu, H. J., and Lennartz, B. (2019), Hydraulic properties of peat soils along a bulk density gradient-A meta study. Hydrological Processes, 33(1), 101-114. doi:10.1002/hyp.13314

McGuire, A. D., Koven, C., Lawrence, D. M., Clein, J. S., Xia, J. Y., Beer, C., . . . Zhuang, Q. L. (2016), Variability in the sensitivity among model simulations of permafrost and carbon dynamics in the permafrost region between 1960 and 2009. Global Biogeochemical Cycles, 30(7), 1015-1037. doi:10.1002/2016gb005405.

McGuire, A. D., et al. (2018), Dependence of the evolution of carbon dynamics in the northern permafrost region on the trajectory of climate change, Proceedings of the National Academy of Sciences of the U. S. A., 115(15), 3882-3887.

McNamara, J. P., D. L. Kane, and L. D. Hinzman (1997), Hydrograph separations in an Arctic watershed using mixing model and graphical techniques, Water Resources Research, 33(7), 1707-1719, doi: 10.1029/97wr01033.

Morris, P. J., Baird, A. J., Eades, P. A., and Surridge, B. W. J. (2019), Controls on Near-Surface Hydraulic Conductivity in a Raised Bog. Water Resources Research, 55(2), 1531-1543. doi:10.1029/2018wr024566

Neilson, B. T., M. B. Cardenas, M. T. O'Connor, M. T. Rasmussen, T. V. King, and G. W. Kling (2018), Groundwater Flow and Exchange Across the Land Surface Explain Carbon Export Patterns in Continuous Permafrost Watersheds, Geophysical Research Letters, 45(15), 7596-7605, doi: 10.1029/2018gl078140.

Nicolsky, D. J., Romanovsky, V. E., and Panteleev, G. G. (2009), Estimation of soil thermal properties using in-situ temperature measurements in the active layer and permafrost. Cold Regions Science and Technology, 55(1), 120-129. doi:10.1016/j.coldregions.2008.03.003

Nicolsky, D. J., Romanovsky, V. E., Panda, S. K., Marchenko, S. S., and Muskett, R. R. (2017), Applicability of the ecosystem type approach to model permafrost dynamics across the Alaska North Slope, Journal of Geophysical Reseach- Earth Surface, 122, 50- 75, doi:10.1002/2016JF003852.

O'Connor, M. T. (2019), Controls Governing Active Layer Thermal Hydrology: How Predictable Subsurface Properties Influence Thaw, Groundwater Flow, and Soil Moisture, 218 pp, The University of Texas at Austin.

O'Connor, M. T., M. B. Cardenas, B. T. Neilson, K. D. Nicholaides, and G. W. Kling (2019), Active Layer Groundwater Flow: The Interrelated Effects of Stratigraphy, Thaw, and Topography, Water Resources Research, 55(8), 6555-6576, doi: 10.1029/2018wr024636.

Painter, S. L., Coon, E. T., Atchley, A., Berndt, M., Garimella, R., Moulton, D., et al. (2016). Integrated surface/subsurface permafrost thermal hydrology: Model formulation and proof-of-concept simulations. Water Resources Research. https://doi.org/10.1002/2015WR018427

Payne, J. (2013), NSSI Landcover Report: Landcover Mapping for North Slope of Alaska, edited, United States Bureau of Land Management.

Ping, C. L., G. J. Michaelson, M. T. Jorgenson, J. M. Kimble, H. Epstein, V. E. Romanovsky, and D. A. Walker (2008), High stocks of soil organic carbon in the North American Arctic region, Nature Geoscience, 1(9), 615-619.

Plaza, C., et al. (2019), Direct observation of permafrost degradation and rapid soil carbon loss in tundra, Nature Geoscience, 12(8), 627-+, doi: 10.1038/s41561-019-0387-6.

Quinton, W. L., M. Hayashi, and S. K. Carey (2008), Peat hydraulic conductivity in cold regions and its relation to pore size and geometry, Hydrological Processes, 22(15), 2829-2837.

Schaefer, K., H. Lantuit, V. E. Romanovsky, E. A. G. Schuur, and R. Witt (2014), The impact of the permafrost carbon feedback on global climate, Environmental Research Letters, 9(8).

Schindler, U., W. Durner, G. von Unold, L. Mueller, and R. Wieland (2010), The evaporation method: Extending the measurement range of soil hydraulic properties using the air-entry pressure of the ceramic cup, Journal of Plant Nutrition and Soil Science, 173(4), 563-572.

Schuur, E. A. G., et al. (2015), Climate change and the permafrost carbon feedback, Nature, 520(7546), 171-179.

Serreze, M. C., and R. G. Barry (2011), Processes and impacts of Arctic amplification: A research synthesis, Global and Planetary Change, 77(1-2), 85-96.

Shiklomanov, N. I., Streletskiy, D. A., Nelson, F. E., Hollister, R. D., Romanovsky, V. E., Tweedie, C. E., et al. (2010). Decadal variations of active-layer thickness in moisture-controlled landscapes, Barrow, Alaska. Journal of Geophysical Research: Biogeosciences, 115(G4), G00I04. https://doi.org/10.1029/2009JG001248

Sjöberg, Y., Coon, E., K. Sannel, A. B., Pannetier, R., Harp, D., Frampton, A., et al. (2016). Thermal effects of groundwater flow through subarctic fens: A case study based on field observations and numerical modeling. Water Resources Research, 52(3), 1591–1606. https://doi.org/10.1002/2015WR017571

Stow, D. A., et al. (2004), Remote sensing of vegetation and land-cover change in Arctic Tundra Ecosystems, Remote Sensing of Environment, 89(3), 281-308.

Tian, Z. C., Gao, W. D., Kool, D., Ren, T. S., Horton, R., and Heitman, J. L. (2018), Approaches for Estimating Soil Water Retention Curves at Various Bulk Densities With the Extended Van Genuchten Model. Water Resources Research, 54(8), 5584-5601. doi:10.1029/2018wr022871

van Genuchten, M. T. (1980), A closed-form equation for predicting the hydraulic conductivity of unsaturated soils, Soil Science Society of America Journal, 44(5), 892-898.

Walker, D. A., and K. R. Everett (1991), Loess Ecosystems of Northern Alaska - Regional Gradient and Toposequence at Prudhoe Bay, Ecological Monographs, 61(4), 437-464.

Walker, D. A., and M. D. Walker (1996), Terrain and vegetation of the Imnavait Creek watershed, in Landscape Function and Disturbance in Arctic Tundra, edited by J. F. R. J. D. Tenhunen, pp. 73-108, Springer.

Walker, D. A., et al. (2003), Vegetation-soil-thaw-depth relationships along a Low-Arctic bioclimate gradient, Alaska: Synthesis of information from the ATLAS studies, Permafrost and Periglacial Processes, 14(2), 103-123.

Walker, D. A., et al. (2018), Circumpolar Arctic Vegetation Classification, Phytocoenologia, 48(2), 181-201.

Xie, X. T., Lu, Y. L., Ren, T. S., and Horton, R. (2018), An empirical model for estimating soil thermal diffusivity from texture, bulk density, and degree of saturation. Journal of Hydrometeorology, 19(2), 445-457. doi:10.1175/jhm-d-17-0131.1

Yumashev, D., Hope, C., Schaefer, K., Riemann-Campe, K., Iglesias-Suarez, F., Jafarov, E., . . . Whiteman, G. (2019), Climate policy implications of nonlinear decline of Arctic land permafrost and other cryosphere elements. Nature Communications, 10. doi:10.1038/s41467-019-09863-x

Figure captions

Figure 1. General and specific location maps of the study sites with land cover types. The Arctic Foothills region of the Alaskan North Slope is indicated by the yellow shade in the inset in (a); the purple box around (a), corresponds to the purple box in the inset map. The red box in (a) corresponds to the area shown in (b). The yellow and black dots in (a) and (b) are locations of soil pits for determination of soil characteristics and strata thickness, and from where samples were collected for laboratory analysis. (c) depicts a typical block of soil taken from a small soil pit showing the acrotelm, catotelm, and mineral soil strata. Note the breadknife for scale.

Figure 2. Mapped thicknesses of the acrotelm (top row) and catotelm (bottom row) grouped by landscape zone (first column), vegetation cover type (second column), and the combined landscape and vegetation category (third column). Boxes represent the interquartile range of each dataset and the brown line represents the median value. Note that tussocks are only present on the hillslope, and tussock acrotelm thickness varies based on microtopographic position (local low vs. local high).

Figure 3. Results of laboratory measurements for samples from acrotelm, catotelm, transitional (organic-rich) mineral, and homogeneous (organic-poor) mineral soil strata. Basic soil properties for each stratum including porosity ϕ, bulk density ρ_b, van Genuchten α, hydraulic conductivity K_H, and thermal conductivity K_T. Boxes represent the interquartile range of each dataset and the red line represents the median.

Figure 4. Correlation of different soil properties with dry bulk density. The plots also show fitted empirical models (red line with corresponding best-fit equation and R^2 value in red font).

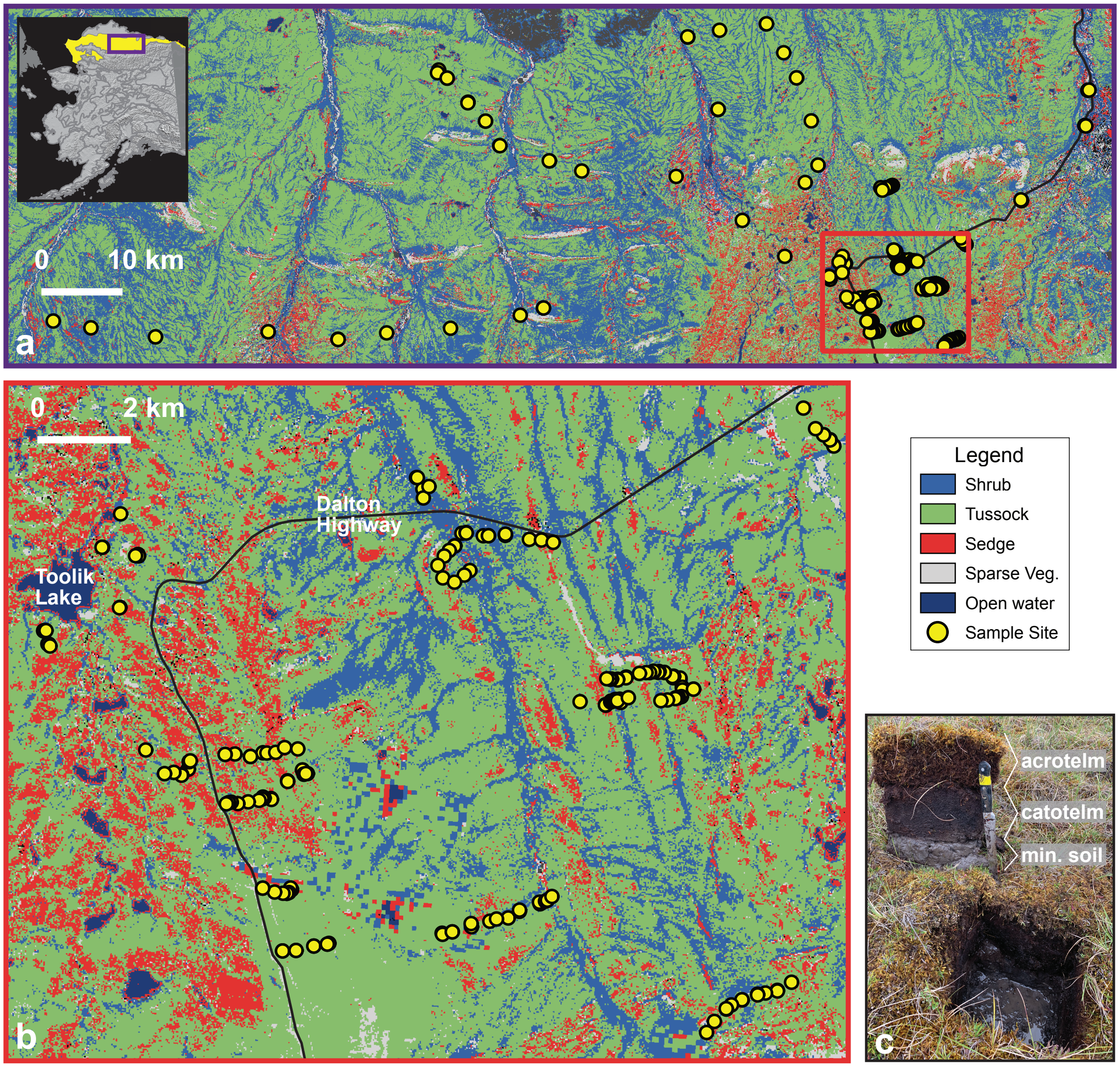
0 10 km
a
0 2 km
Dalton Highway
Toolik Lake
b
Legend
Shrub
Tussock
Sedge
Sparse Veg.
Open water
Sample Site
acrotelm
catotelm
min. soil
c

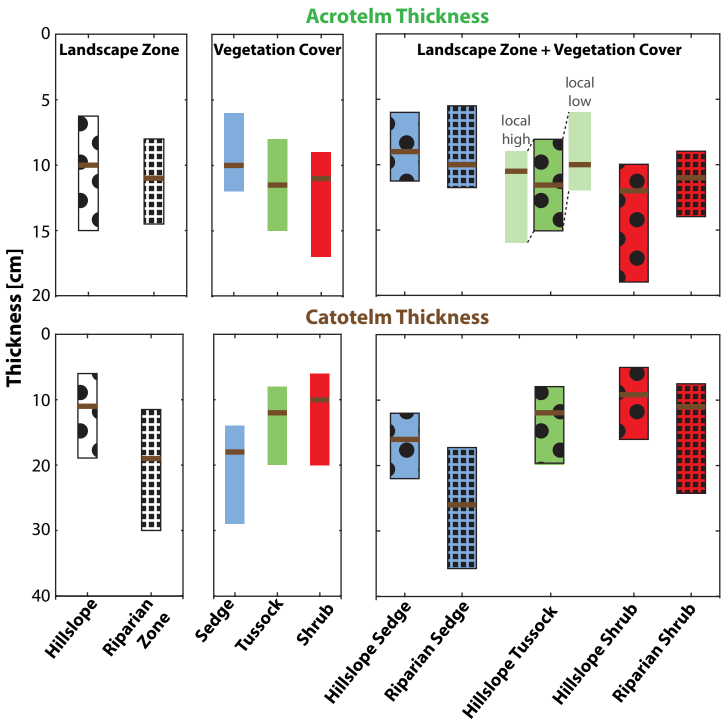
Acrotelm Thickness
Landscape Zone
Vegetation Cover
Landscape Zone + Vegetation Cover
local high
local low
0
5
10
15
20
Thickness [cm]
Catotelm Thickness
0
10
20
30
40
Hillslope
Riparian Zone
Sedge
Tussock
Shrub
Hillslope Sedge
Riparian Sedge
Hillslope Tussock
Hillslope Shrub
Riparian Shrub

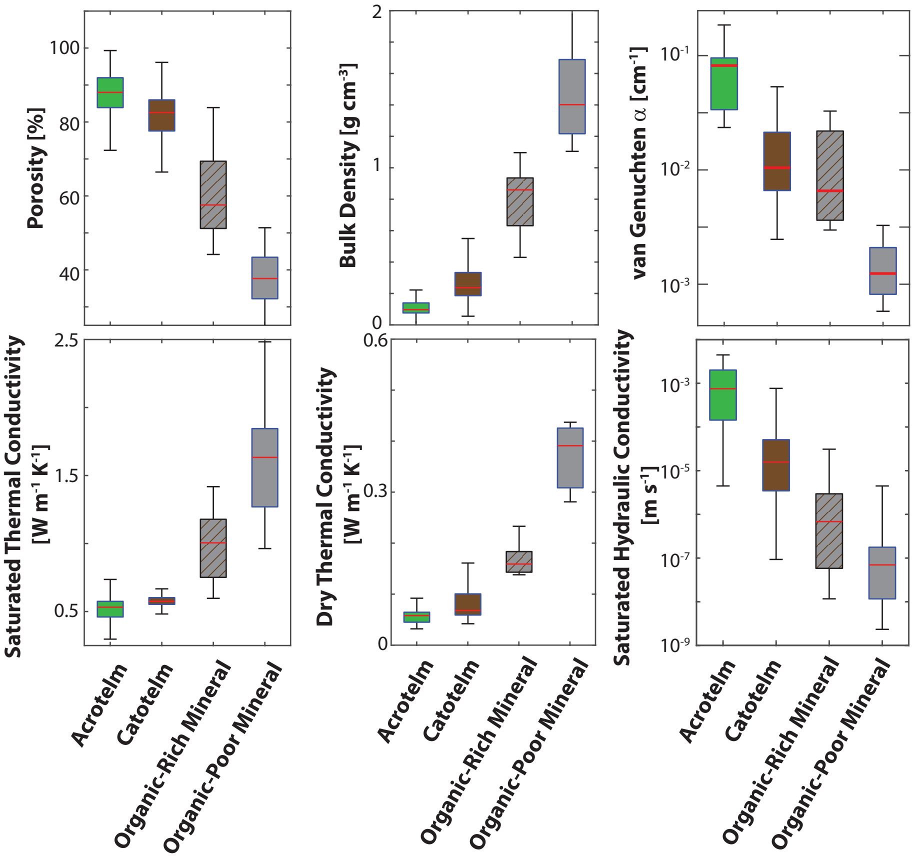
Porosity [%]
100
80
60
40
Bulk Density [g cm^{-3}]
2
1
0
van Genuchten α [cm^{-1}]
10^{-1}
10^{-2}
10^{-3}
Saturated Thermal Conductivity [W m^{-1} K^{-1}]
2.5
1.5
0.5
Dry Thermal Conductivity [W m^{-1} K^{-1}]
0.6
0.3
0
Saturated Hydraulic Conductivity [m s^{-1}]
10^{-3}
10^{-5}
10^{-7}
10^{-9}
Acrotelm
Catotelm
Organic-Rich Mineral
Organic-Poor Mineral
Acrotelm
Catotelm
Organic-Rich Mineral
Organic-Poor Mineral
Acrotelm
Catotelm
Organic-Rich Mineral
Organic-Poor Mineral

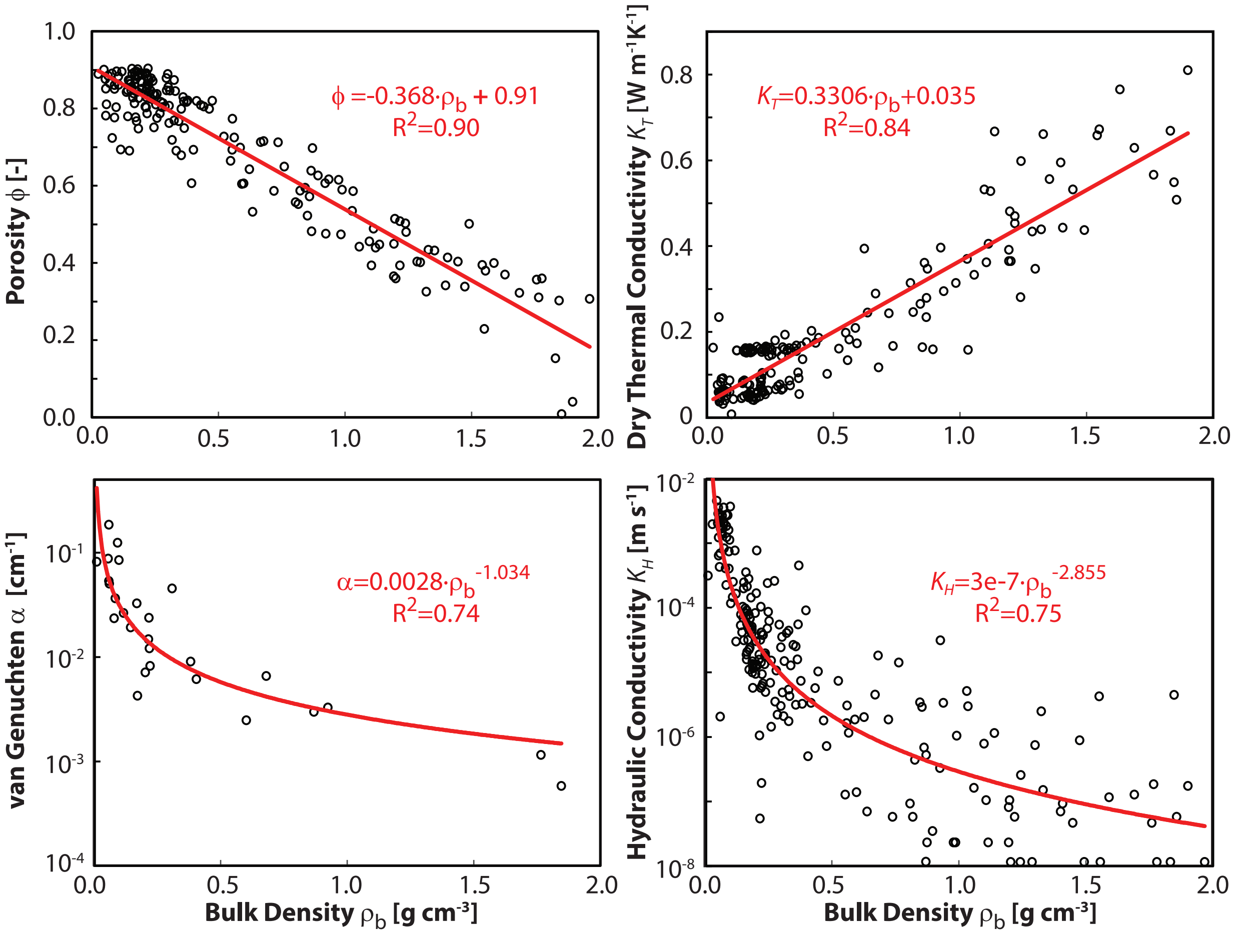
Porosity ϕ [-]
1.0
0.8
0.6
0.4
0.2
0.0
$\phi = -0.368 \cdot \rho_b + 0.91$
$R^2 = 0.90$
0.0
0.5
1.0
1.5
2.0
Dry Thermal Conductivity K_T [W m^{-1}K^{-1}]
0.8
0.6
0.4
0.2
0
$K_T = 0.3306 \cdot \rho_b + 0.035$
$R^2 = 0.84$
0.0
0.5
1.0
1.5
2.0
van Genuchten α [cm^{-1}]
10^{-1}
10^{-2}
10^{-3}
10^{-4}
$\alpha = 0.0028 \cdot \rho_b^{-1.034}$
$R^2 = 0.74$
0.0
0.5
1.0
1.5
2.0
Bulk Density ρ_b [g cm^{-3}]
Hydraulic Conductivity K_H [m s^{-1}]
10^{-2}
10^{-4}
10^{-6}
10^{-8}
$K_H = 3e{-}7 \cdot \rho_b^{-2.855}$
$R^2 = 0.75$
0.0
0.5
1.0
1.5
2.0
Bulk Density ρ_b [g cm^{-3}]